SLAC – PUB – 4361
July 1987
(E)

J/ψ AND Υ RADIATIVE AND HADRONIC DECAYS*

Elliott D. Bloom
Stanford Linear Accelerator Center
Stanford, California 94305

Invited talk presented at
Les Rencontres de Physique
de la Vallee D'Aoste
LaThuille, Aosta Vallee, Italy
March 1–7, 1987

* Work supported by the Department of Energy, contract DE – AC03 – 76SF00515.

1. Introduction

After 12 years of data at the $c\bar{c}$ system and almost as long at the $b\bar{b}$ system, there still is much interesting physics emerging, and much left to do. In this report I will discuss only a small subset of the physics results continuing to flow from studies of the $c\bar{c}$ and $b\bar{b}$ resonances, those concerned with the search for gluonium at the J/ψ and Υ, and the search for "exotics" at the Υ. In addition, I will briefly touch on future perspectives.

Figure 1 gives a brief overview of the spectroscopy of the charmonium and bottomonium systems. All of the different spin - parity states have been observed, in one system or the other, except perhaps for the $^1P_1$. Weak evidence exists for the $^1P_{1c}$ state in $p\bar{p}$ collisions[1]. The n^1S_{0b} states (η_b) have not yet been observed. The figure also schematically indicates the reactions to be discussed in this report, radiative and hadronic decays of the J/ψ, and the search for radiative decays of the Υ.

The study of exclusive hadronic decays of the J/ψ, primarily by the Mark III collaboration[2], has shed considerable light on the character of the states seen in J/ψ radiative decays. In addition, recent results from the TPC/2γ experiment[3] on $\gamma\gamma$ interactions, and the LASS spectrometer[4] observing K^-p interactions, has further helped untangle the low mass meson spectrum. The questions concerning the gluonic character of some of these states, i.e., glueball or not, has consequently made real progress.

The radiative decays from the Υ[5] have been used together with those from the J/ψ[6] to put stringent limits on both the standard and nonstandard axions. However, other topics deriving from radiative decays from the Υ are presently in a relatively primitive state. Only limits exist for radiative decays to hadrons, and searches for "exotic" states are just getting started. As I will show, even searches for a light higgs are not yet close to excluding standard model branching ratios over most of the mass range experimentally accessible in the Υ system of about 0 GeV to 10 GeV.

2. The Search for Gluonium

2.1 PHENOMENOLOGY

The process,

$$J/\psi \rightarrow gg + \gamma, \tag{1}$$

where the to gluons fragment to hadrons, is given in lowest order QCD[7] by the expression,

$$(1/\Gamma_{\rm had})\mathrm{d}\Gamma/\mathrm{d}x(Q\overline{Q} \rightarrow \gamma + \text{hadrons}) \simeq 0.12(0.2/\alpha_S)\left(\frac{e_Q/e}{2/3}\right)^2 \mathrm{d}N^0/\mathrm{d}x. \tag{2}$$

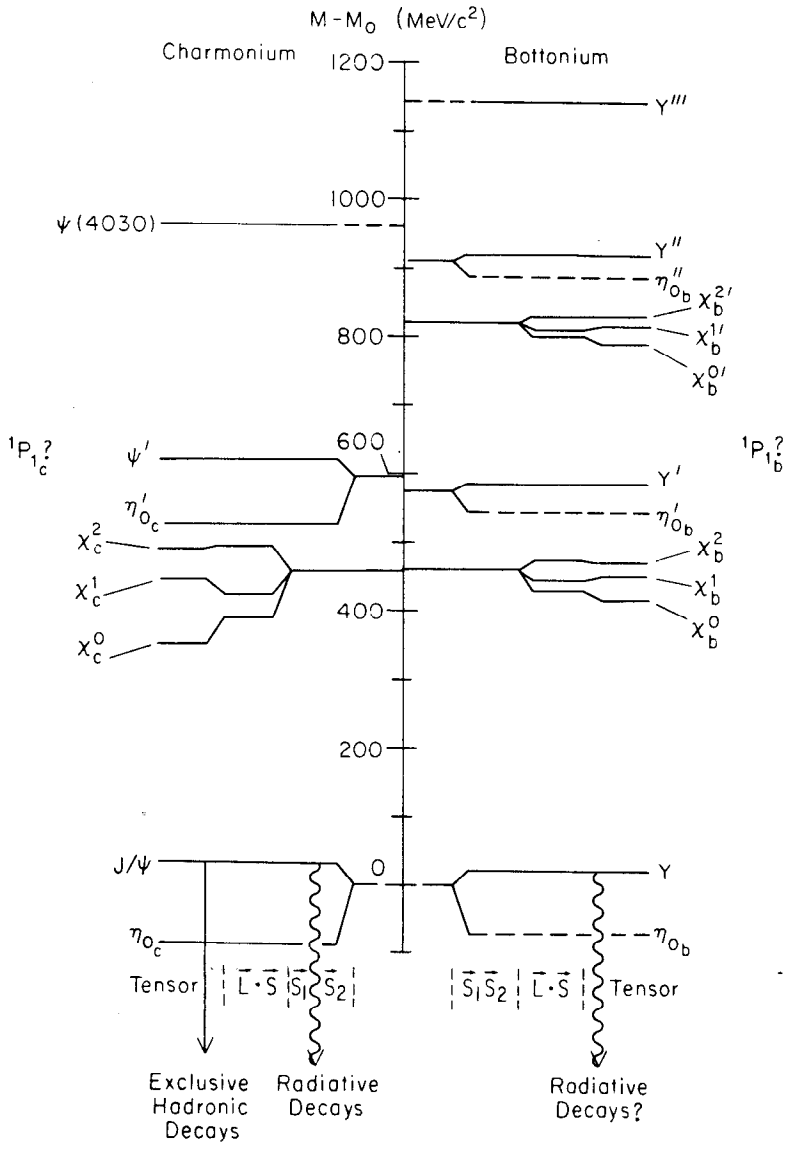

Figure 1. Level diagram, with mass differences and spin splitting for charmonium and bottomonium. The observed states are shown as solid lines. The $^1P_1$ states are not shown. The topic of this report is schematically indicated at the bottom of the diagram along with a legend for the spin splitting.

The dN^0/dx factor is typically taken from QED[8] for use in the scaling region,

$$dN^0/dx = \frac{2}{(\pi^2-9)}\left[\frac{x(1-x)}{(2-x)^2} - \frac{2(1-x)^2}{(2-x)^3}\ln(1-x) + \frac{(2-x)}{x} + \frac{2(1-x)}{x^2}\ln(1-x)\right], \tag{3}$$

$$\text{and,} \qquad x \equiv \frac{2E_\gamma}{M_{Q\overline{Q}}}.$$

Figure 2a shows a comparison of the data from the Mark II experiment[9] at the J/ψ with the above equations. The data is clearly softer than the theory near $x = 1$. Figure 2b shows a comparison of CUSB data[10] at the Υ with the above equations; the agreement is remarkably good. Results from CLEO[11] do not compare as well, again being softer than the theory near $x = 1$. In all cases, the integral of the data extrapolated to $x = 0$ agrees with the theory within error,

$$B(J/\psi \to \gamma + \text{hadrons}) \simeq 12\%, \qquad \text{(Mark II)}, \tag{4}$$

$$B(\Upsilon \to \gamma + \text{hadrons}) \simeq 3\%, \qquad \text{(CUSB, CLEO)}.$$

Note that in both cases the resolution function of the detector appreciably modifies the theoretical scaling curve (shown as the solid line in both parts of the figure) near $x = 1$. The unmodified theoretical curve is monotonically increasing from $x = 0$ to $x = 1$.

Figure 3 shows preliminary results from the crystal ball experiment at the J/ψ. The superior photon resolution of this NaI(tl) device has allowed the observation of the resonance structures in the photon inclusive spectrum. Unfortunately, the spectrum shown is not normalized, and is only useful in revealing structure. The difficulty in obtaining an absolute cross section lies in calculating the photon detection efficiency associated with the low multiplicity final states of the resonances, many of which are unknown.

One is interested in "scaling" the resonances from the J/ψ inclusive photon spectrum, e.g., as in figure 3, to the Υ. Later in this report we will compare results form the J/ψ to those at the Υ. How to make this comparison is problematic as, clearly, the data is not in the scaling region for the J/ψ, and may not be for the Υ (though the CUSB result suggests it may be). One can get some idea of what to expect at the Υ from the J/ψ data by using a "local duality" argument reminiscent of that used for deep inelastic electron scattering[12],

$$\Gamma(V \to \gamma + gg(\to m)) \sim e_V^2\,\alpha_S^2\,\frac{|R(0)|^2}{M_V^2}\int_{\Delta x} \mathrm{F}(x)\,dx,$$

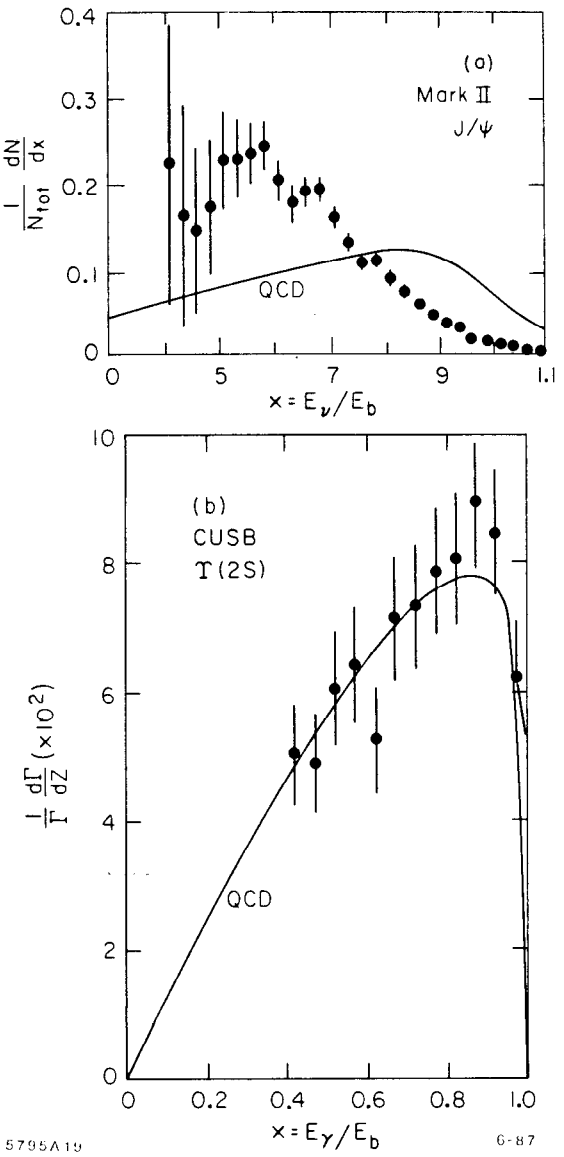

Figure 2. Comparison of data and theory with experimental resolution folded in for the process, a) $J/\psi \to \gamma + X$, Mark II data[9] b) $\Upsilon \to \gamma + X$, CUSB data[10].

$$\text{where,} \qquad x \equiv \frac{2E_\gamma}{M_V} = 1. - m^2/M_V^2,$$

and Δx is the photon energy bite corresponding to the total energy width of the produced meson m. $\mathrm{F}(x)$ is the scaling function, approximated by $\mathrm{d}N^0/\mathrm{d}x$ given previously. This has been typically what has been done[13]. However, if one can believe the data there are obvious corrections to this simple scaling argument; the data at the J/ψ are not yet in the scaling region. Thus using the data itself at the J/ψ, i.e. $\mathrm{F}(x) \rightarrow \mathrm{F}(x,m)$, and assuming scaling at the Υ, one finds,

$$\frac{B(\Upsilon \rightarrow \gamma + m)}{B(J/\psi \rightarrow \gamma + m)} \simeq \left(\frac{\alpha_s(\Upsilon)}{\alpha_s(J/\psi)}\right)^2 \left(\frac{M_{J/\psi}}{M_\Upsilon}\right)^2 \left(\frac{B_{ee}^\Upsilon}{B_{ee}^{J/\psi}}\right) \frac{\mathrm{d}N^0/\mathrm{d}x\,|_\Upsilon^m}{\mathrm{F}(x,m)|_{J/\psi}^m}. \tag{6}$$

The first three factors on the right of the above equation lead to the usual prediction of a factor of about 40 reduction in the Υ rate for a state of mass m as compared to the J/ψ. However, the last factor in the equation, call it Y, modifies this simple result in a major way and with some uncertainty due to the large errors of the data.

The results of a calculation using these local duality ideas is given in table 1 below. We will compare with experiments in the section which discusses the search for Υ radiative decays.

Table 1

State m	Mass (GeV)	x^Υ	$x^{J/\psi}$	Y	$\frac{B(\Upsilon\rightarrow\gamma+m)}{B(J/\psi\rightarrow\gamma+m)}$
η	0.548	0.997	0.969	5.6	0.16
η'	0.958	0.990	0.904	3.7	0.10
f	1.270	0.982	0.832	2.6	0.07
ι	1.440	0.977	0.783	1.3	0.04
f'	1.525	0.974	0.757	1.3	0.04
θ	1.720	0.967	0.691	0.7	0.02

Past attempts to determine which of the prominent states seen in J/ψ radiative decays might be gluonium states, or have large gluonium admixtures in their wave functions, have not been successful in the view of many. Recently, the Mark III collaboration has developed a phenomenolgical approach to this problem which has led to progress, and may ultimately allow a reliable identification of major gluonium states.

Figure 4 schematically shows the Mark III methodology[2]. Parts a) and b) of the figure display the nominal competing mechanisms in J/ψ radiative decay. Part a) shows decays to

normal mesons, b) shows decays to states with a large gluonium content. The Mark III uses related hadronic decays to determine if a candidate gluonium state behaves as a $q\bar{q}$ state or not. If the state does not behave as expected for a $q\bar{q}$ state, one might strongly suspect a large gluonium admixture. Part c) indicates the decay of the candidate state with a ϕ meson, part d) decay with an ω meson , and part e) through a doubly OZI suppressed mechanism (DOZI). Parts c) and d) of the figure allow a "flavor tagging" of the decay, assuming part e) is not important in the decay process. Decays to glueballs should not show large rates via the mechanisms of figures c) and d).

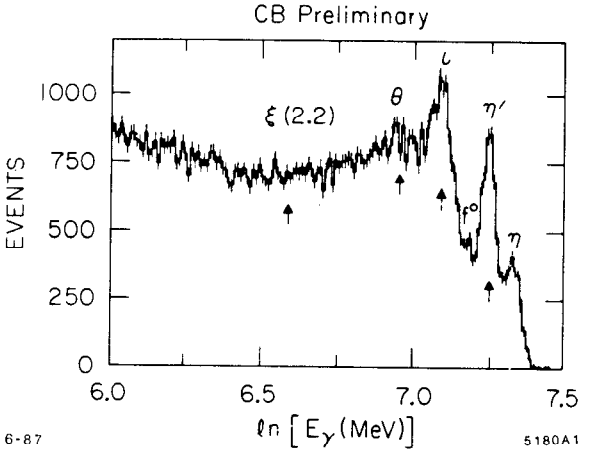

Figure 3. Preliminary crystal ball collaboration data for the process $J/\psi \rightarrow \gamma + X$, emphasizing the resonance region.

2.2 The Status of the $\iota(1440)$ (or $\eta(1440)$).

Always suspected of being a glueball, the character of this $J^P = 0^-$ state has been contested since its discovery about 7 years ago. The confusion has become particularly intense since the J^P of the $E(1420)$, nominally a member of the 1^+ nonet, has recently been questioned[14]. The mass region of these states is complex with Meikton $(q\bar{q}g)$[15] as well as $q\bar{q}$ and gg theoretical predictions abounding. I am thus happy to report that there seems to be some relief in sight. A number of recent experimental results suggest that a reasonable understanding of the 1400–1500 MeV/c^2 mass range may be in reach.

Figures 5 and 6 show recent results from the Mark III collaboration[2]. Figure 5 concentrates on the $K\overline{K}\pi$ decay modes in various final states Part a) of the figure shows the combined signal in $\gamma K\overline{K}\pi$ from their recent high statistics J/ψ sample (about 5×10^6 hadronic decays). This is the classical way to see the ι. The Mark III finds after a multichannel analysis including the Dalitz plot,

$$M_\iota = 1458 \pm 5 \pm 6 \text{ MeV/c}^2, \quad \Gamma = 98 \pm 10 \pm 10 \text{ MeV/c}^2, J^P = 0^-,$$

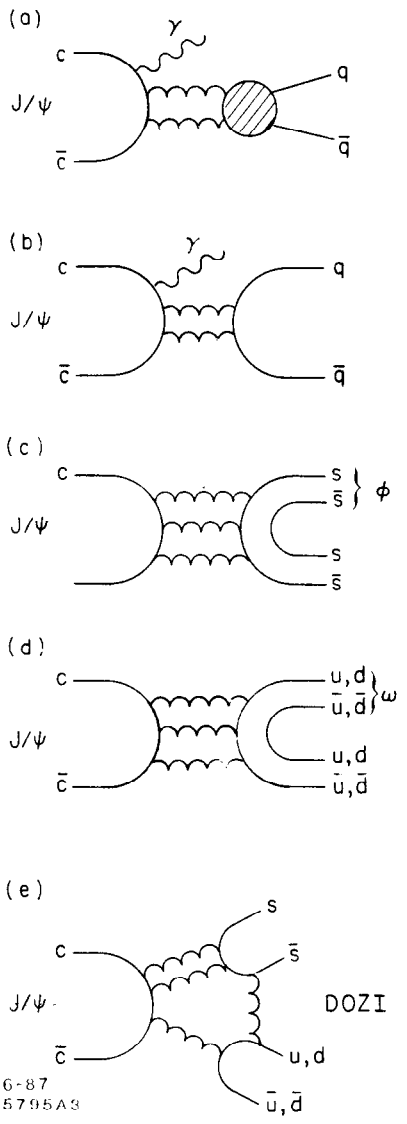

Figure 4. Diagramatic explanation of the Mark III methodology for untangling the gg and $q\bar{q}$ spectroscopy in J/ψ radiative decays: Part a), radiative decay to a gluonium final state; part b), radiative decay to a $q\bar{q}$ final state; part c), quasi two body decay to a ϕ and the $s\bar{s}$ part of a meson; part d), quasi two body decay to a ω and the $(u\bar{u}+d\bar{d})$ part of a meson; part e), doubly OZI suppressed decay (DOZI).

(7)

$$B(J/\psi \to \gamma + \iota) \times B(\iota \to K\overline{K}\pi) = (50 \pm 3.0 \pm 8.0) \times 10^{-4}.$$

Part b) of the figure shows the recoil spectrum against the ω in the decay, $J/\psi \to \omega K\overline{K}\pi$. There is a peak evident in the spectrum at close to the ι mass.

$$M = 1442 \pm 5^{+10}_{-17}\ \mathrm{MeV/c^2}, \quad \Gamma = 40^{+17}_{-13} \pm 5\ \mathrm{MeV/c^2}. \tag{8}$$

The width of this state is not consistent with that of the ι, being too narrow. The insert in figure 5b) shows the distribution of the normal to the ω decay plane in the helicity system of the ω. The solid curve is the Monte Carlo for a $J^P = 0^-$ state. The goodness of fit for the spin 0^- hypothesis is 6%. The Mark III has also done a coupled channel analysis on the $K\overline{K}\pi$ system for this decay[16]. $K\overline{K}^*\pi$ was found to be the dominant contribution with $J^P = 1^+$. A natural interpretation for this structure is thus the E (1420) ($f_1(1420)$) meson produced in association with an ω . No hint of the ι is seen in this channel.

Part c) of the figure shows the decay of the J/ψ to $K\overline{K}\pi$ in association with a ϕ meson. Again no hint of the ι is seen in this channel, as well as no hint of the E meson. Apart from a small signal a 1280 MeV/c^2, the rest of the spectrum is dominated by a broad phase space like distribution. The mass and width of the structure at 1280 MeV/c^2 was measured to be,

$$M = 1279 \pm 6 \pm 10\ \mathrm{MeV/c^2}, \quad \Gamma = 14^{+20}_{-14} \pm 10\ \mathrm{MeV/c^2}. \tag{9}$$

These values are consistent with the $D(1285)$, an isosinglet member of the 1^{++} nonet. A detail of the 1200 MeV/c^2 mass region after a selecting $M(K\overline{K}) < 1150$ MeV/c^2 (a δ cut) is shown in the insert to part c).

On contemplating the results of the discussion of figure 5 a few somewhat tentative conclusions emerge. Firstly, the ι is not $q\overline{q}$; secondly, the $E(1440)$ is not pure $s\overline{s}$ as previously assumed, i.e., the 1^{++} octet is not ideally mixed; finally, the $D(1285)$ has some $s\overline{s}$ content, which seems a necessary condition for the previous conclusion.

Figure 6 continues the story with the examination of decays of the type, $J/\psi \to X\eta\pi\pi, X = \gamma, \omega, \phi$. Part a) shows the $\eta\pi^+\pi^-$ mass spectrum recoiling against a γ after a δ cut. The latter emphasizes the 1200 $\sim$ 1600 MeV/c^2 region. A narrow peak at $\sim$ 1280 MeV/c^2 and another at $\sim$ 1390 MeV/c^2 are apparent. The lower peak at 1285 MeV/c^2 is consistent with the D, however, it is also consistent with the $\eta(1275)$[17]. The second peak occurs at a mass lower than the nominal ι mass. The Mark III states[2] that a complete partial wave analysis is needed to clarify the situation.

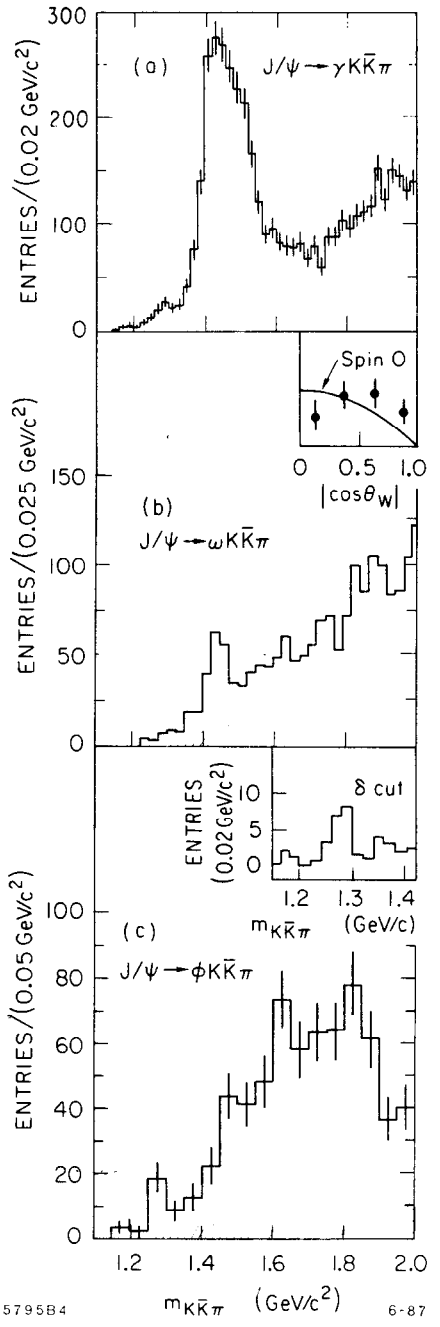

Figure 5. Mark III mass spectra[2] showing $K\overline{K}\pi$ recoiling against: Part a), a γ; part b), a ω; part c), a ϕ. The insert in part b) shows the angular distribution of the recoil ω compared to a $J^P = 0^-$ hypothesis for the $K\overline{K}\pi$ final state structure at 1.44 GeV/c^2. The insert in part c) shows a close-up of the 1.3 GeV/c^2 region after a δ cut.

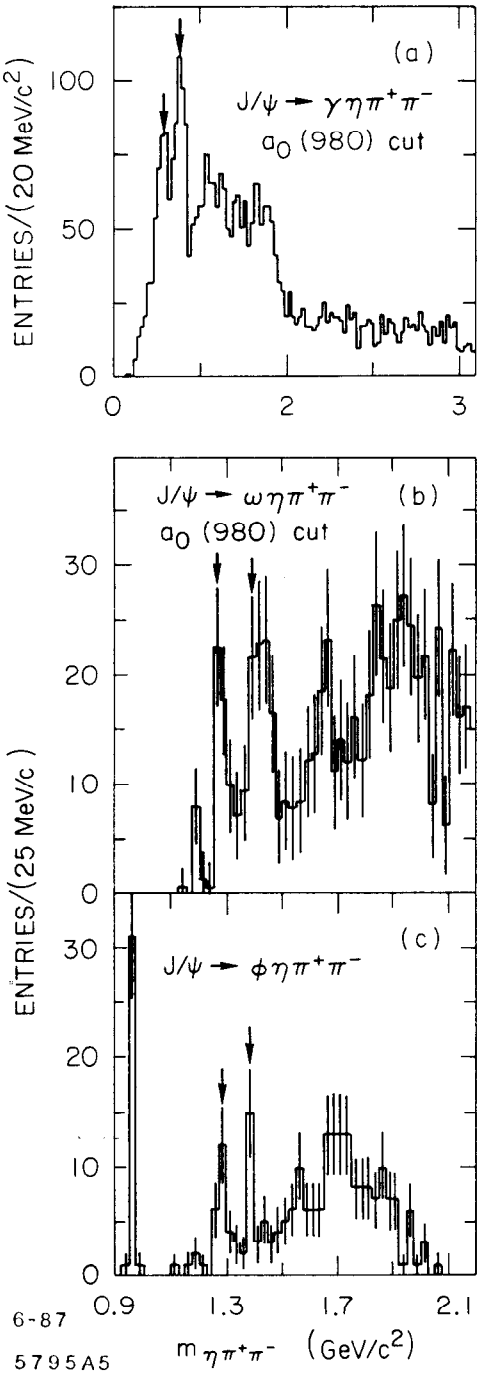

Figure 6. The $\eta\pi^+\pi^-$ (background subtracted) invariant mass spectra from the reactions: a) $J/\psi \to \gamma\eta\pi^+\pi^-$; b) $J/\psi \to \omega\eta\pi^+\pi^-$; $J/\psi \to \phi\eta\pi^+\pi^-$; all spectra from the Mark III collaboration[2].

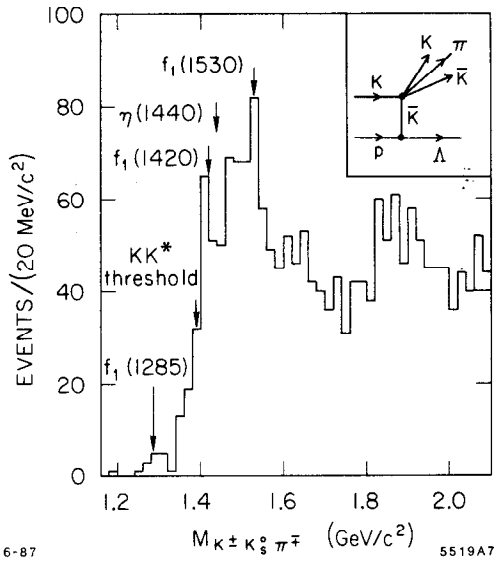

Figure 7. LASS[4] $K_s K^{\pm}\pi^{\mp}$ invariant mass spectrum from 11 GeV/c^2 $K^- p \to K_s K^{\pm}\pi^{\mp}\Lambda$.

Part b) shows the $\eta\pi^+\pi^-$ recoiling against an ω also after a δ cut. The statistics are poor, but a consistent picture emerges with peaks at the D and E, a fit to the higher mass bump yielding (before the δ cut),

$$M = 1421 \pm 8 \pm 10 \text{ MeV/c}^2, \quad \Gamma = 45^{+32}_{-23} \pm 15 \text{ MeV/c}^2. \tag{10}$$

Part c) shows the result for $X = \phi$. A large η is signal seen at the low end of the spectrum. At $M \sim 1285$ MeV/c^2, there is a peak compatible with the D. Again, the ι and the E do not appear convincingly in the spectrum; a possible narrow structure is seen at ~ 1400 MeV/c^2; however, only a single high bin is observed. Some of the tentative conclusions drawn above are somewhat more strongly supported by the discussion of figure 6. The D and E seem to both have some $s\bar{s}$ as well as $(u\bar{u} + d\bar{d})$ content, and so it is unlikely that the 1^{++} nonet is ideally mixed. As the ι has little branching fraction into the $\eta\pi\pi$ final state, not much is added by the results shown in figure 6 to the nature of this state. However, recent results from the LASS spectrometer at SLAC seem to bear on the nature of the ι.

Figure 7 shows recent results from LASS[4] for the reaction,

$$K^- p \to K_s K^{\pm}\pi^{\mp}\Lambda. \tag{11}$$

The invariant mass spectrum for the $K^{\pm}K_s\pi^{\mp}$ final state is shown in the figure. As well as other structure, there is an indication for the $E(1420)$ in the figure; however, there is no indication for the ι in the figure. This result confirms the Mark III result of figure 5 indicating that the ι does not behave like a $q\bar{q}$ state.

Additional information on this complex mass region has been obtained through the study of $\gamma\gamma$ interactions. In particular, recent results from the TPC/2γ collaboration at PEP have been enlightening. The particle identification of the TPC has been useful in these studies, and figure 8 shows an up to date calibration of the TPC dE/dx system and the spectacular particle separation obtained. The data shown have a dE/dx resolution with a σ of 3.6%.

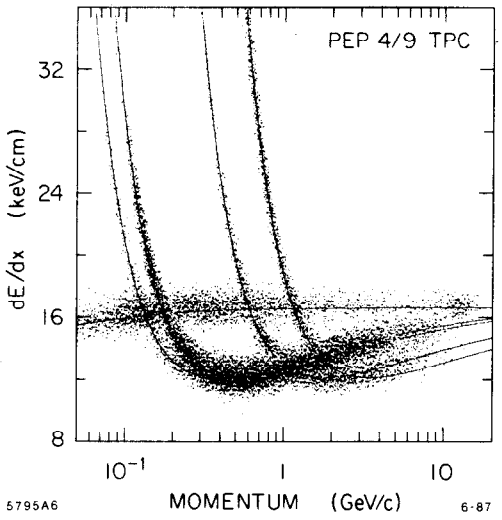

Figure 8. dE/dx spectra from the TPC/2γ collaboration[3]. The resolution is $\sigma/(dE/dx) = 3.6\%$.

One of the reactions studied was,

$$\gamma\gamma \rightarrow K_s K^{\pm}\pi^{\mp}. \tag{12}$$

However, using the endcap spectrometers of the detector allowed a tuning of q^2 for one of the incident virtual γs. Thus both on shell and off shell (for the γ) production of resonances in the 1.4 GeV/c^2 mass region was measured. Figure 9a shows the $K_s K^{\pm}\pi^{\mp}$ invariant mass distribution for the on shell $\gamma\gamma$ reaction. No structure is seen in the data (black histogram). The dotted histogram has the shape of an ι signal which should have been seen if

$$\Gamma_{\iota\rightarrow\gamma\gamma} B(K\overline{K}\pi) = 1.6 \text{ keV} . \tag{13}$$

1.6 keV is the 95% confidence upper limit reported by the TPC/2γ collaboration[3].

Figure 9b shows the results for single tag events in the same channel[3]. (Single tag events have $q^2 > 0.25$ GeV/c^2 for the e^- or e^+.) There is a clear peak of thirteen events in the mass region from 1.3 to 1.6 GeV/c^2. A fit to the peak, assuming a constant background, yields,

$$M = 1417 \pm 13 \text{ MeV/c}^2, \quad \Gamma = 35^{+47}_{-20} \text{ MeV/c}^2. \tag{14}$$

These values are consistent with the $E(1420)$; however, the $\gamma\gamma$ width of, $\Gamma_{\gamma\gamma^*} = 4 \pm 1 \pm 1$ keV, (Preliminary TPC/2γ) , is about a factor of 10 too high to be explained by a primarily $s\bar{s}$

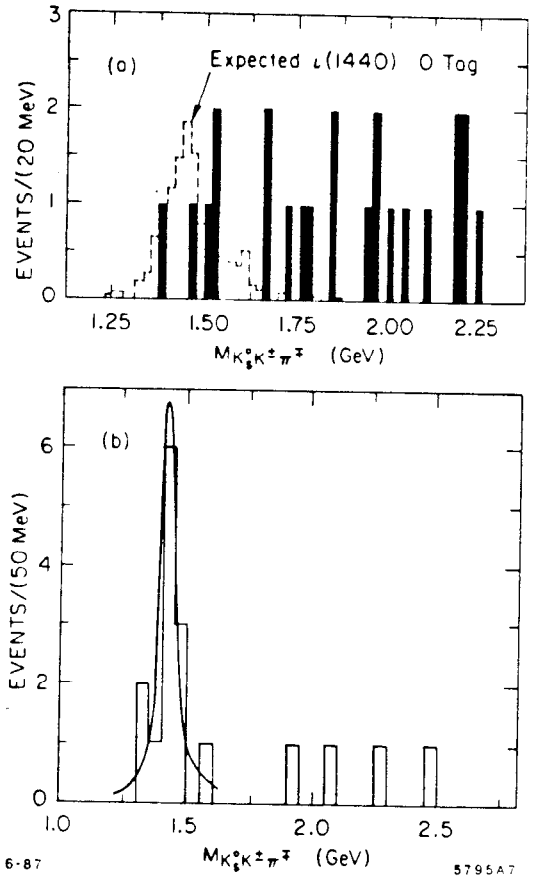

Figure 9. TPC/2γ[3], invariant $K_s K^\pm \pi^\mp$ mass spectra from $\gamma\gamma$ production: part a), no tag $\gamma\gamma$ events ($q^2 \sim 0$); the dotted histogram has the shape of an ι signal which should have been seen if $\Gamma_{\iota \to \gamma\gamma} = 1.6$ keV; part b), single tag events with $q^2 > 0.25$; the solid line is a Monte Carlo calculation for the expected shape of an $E(1420)$ meson with phase space decay.

state[18]. Figure 10 shows the q^2 distribution of $B\Gamma_{\gamma\gamma^*}$, where B is the branching ratio to $K\overline{K}\pi$ with a correction made for the unseen decay modes on the assumption that the resonance has $I = 0$. The data are acceptance corrected for spin 0 in part a) of the figure, and spin 1 for part b). Clearly, the particle is spin 1.

Chanowitz[15] has suggested that this spin 1 state is a Meikton, $J^P = 1^-$. In $\gamma\gamma$ collisions there are effectively two spin combinations of the incoming photons involved in the production cross sections, σ_{TT} and σ_{ST}, where T is a transversely polarized and S is a longitudinally polarized photon. One expects σ_{ST} to dominate in spin 1 production, as ,

$$\sigma_{ST} \propto q^2, \sigma_{TT} \propto q^4, \text{as } q^2 \to O. \tag{15}$$

Preliminary TPC/2γ analysis of the Dalitz plot yields the results of Table 2.

The data are consistent with K^*K dominance, but do not require it.

Table 2

		Probability of a Worse Fit in %			
J^P	Final State	σ_{ST}	σ_{TT}	$\sigma_{ST}, q^2 < 1$(GeV/c^2)	$\sigma_{TT}, q^2 < 1$(GeV/c^2)
1^+	K^*K	86	9	54	11
1^+	$K\overline{K}\pi$	86	1	54	0.9
1^-	K^*K	7	5	12	0.3
1^-	$K\overline{K}\pi$	0.006	2	0.7	3

Thus if σ_{ST} is dominant, $J^P = 1^+$ is favored over 1^-. However, as q^2 approaches M_x^2, σ_{TT} must begin to contribute. A truly definitive answer needs about 10 times the data (which we hope to collect at HighLum PEP).

A reasonably consistent set of conclusions emerge from the various experiments I have discussed on the question of the nature of the ι, and other resonances near the ι in mass:

- The $\iota(1440)$ does not behave like a $q\bar{q}$ state; it is a good candidate for 0^- gluonium.
- After all these years, the 1^{++} nonet assignments looks problematic. In particular, the $D(1285)$ and the $E(1420)$ are not ideally mixed.
- The structure in $\gamma\gamma$ reactions with mass about 1420 is probably the E meson, and not a meikton with $J^P = 1^-$. However, more data is needed to firm up this result.

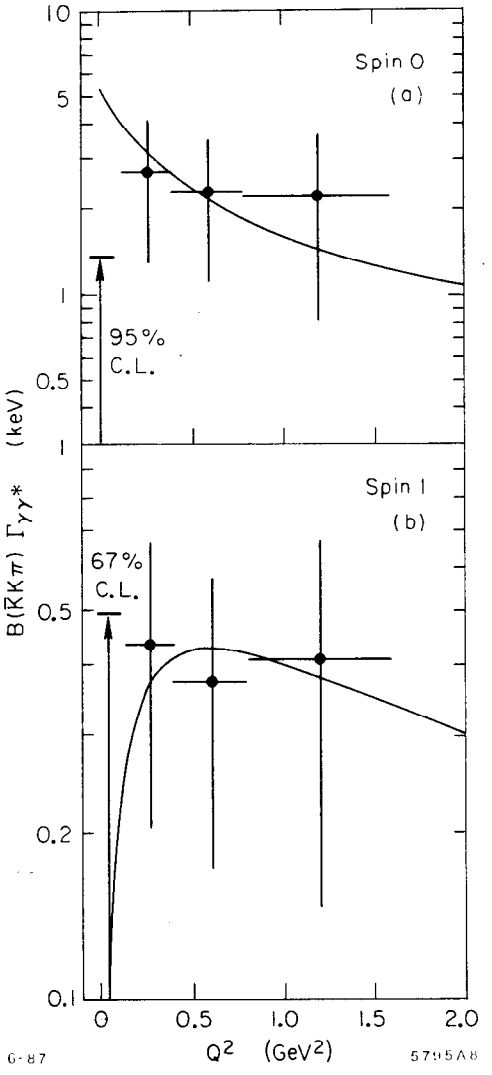

Figure 10. $B(KK\pi)\Gamma_{\gamma\gamma^*}$ from the TPC/2γ collaboration[3], where the data are acceptance corrected with (a) the spin-0 Monte Carlo model and (b) spin-1 Monte Carlo model. The upper limits near $q^2 = 0$ come from no-tag data, where no resonance was seen. The curves are the best fits to the single-tag points of the expected (a) spin-0 and (b) spin-1 q^2 dependence.

2.3 THE STATUS OF THE $\theta(1720)$ (OR $f_2(1720)$).

As the 1700 MeV/c^2 mass region is less crowded, the θ has always been appealing as a 2^{++} gluonium state. Some theoretical controversy has clouded the issue, but the relative simplicity of the spin 2 states seem to leave no room for the θ as a normal $q\bar{q}$ meson. A similar analysis as made for the ι by the Mark III collaboration[2] has also been made for the θ, and this confirms past prejudice. The LASS spectrometer also has new results on this question[4].

Figures 11 and 12 show results from the Mark III on J/ψ decay. Figure 11 considers decays into XK^+K^-, where X is a γ, ω or ϕ. As described earlier, the comparison of a state produced in the radiative decay mode and a similar state produced in hadronic decay modes proves to be a useful tool to differentiate between the gluonic and quark content of the state. From figure 11a) the Mark III obtains,

$$M = 1720 \pm 7 \text{ MeV/c}^2, \quad \Gamma = 132 \pm 15 \text{ MeV/c}^2, \qquad B = (4.8 \pm 0.6 \pm 0.9) \times 10^4. \tag{16}$$

From figure 11 b), they obtain,

$$M = 1731 \pm 10 \pm 10 \text{ MeV/c}^2, \quad \Gamma = 110^{+45}_{-35} \pm 15 \text{ MeV/c}^2, \qquad B = (4.5^{+1.2}_{-1.1} \pm 1) \times 10^4. \tag{17}$$

These parameters are consistent with those of the θ, and show a large branching ratio associated with the ω. Conventional $q\bar{q}$ mesons are not expected to be produced profusely in this final state as only a DOZI mechanism allows it. Part c) of the figure shows K^+K^- production associated with a ϕ. A prominent $f_2'(1525)$ is seen, with a shoulder on the high mass side. A coherent fit with standard f_2' and θ parameters describe the data well. A detailed study by the Mark III is underway, with the proper mix of the angular distributions.

Figure 12 shows the $X\pi^+\pi^-$ final state for $X = \gamma, \omega, \phi$. Part a) shows the invariant $\pi^+\pi^-$ mass spectrum recoiling against a γ. The low mass peak $\sim$ 700 MeV/c^2 is feed-down from the $\phi^0\pi^0$ decay mode of the J/ψ. Along with a strong $f_2(1270)$ signal, and a shoulder possibly due to the $f_2'(1525)$, the θ is clearly observed at the expected mass (arrow in the figure). The Mark III has obtained,

$$M_{\theta\to\pi\pi} = 1713 \pm 15 \text{ MeV/c}^2, \quad \Gamma = 130 \text{ MeV/c}^2 \text{ (fixed)}. \tag{18}$$

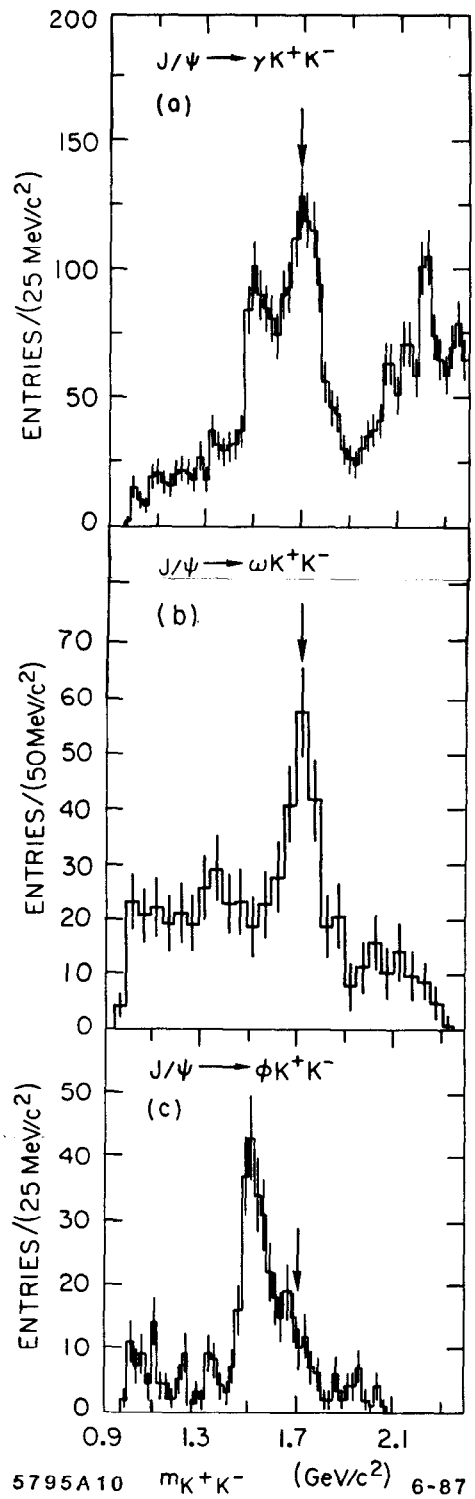

Figure 11. Mark III[2] effective mass spectra in the reactions (a) $J/\psi \to \gamma K^+K^-$, (b) $J/\psi \to \omega K^+K^-$, (c)$J/\psi \to \phi K^+K^-$.

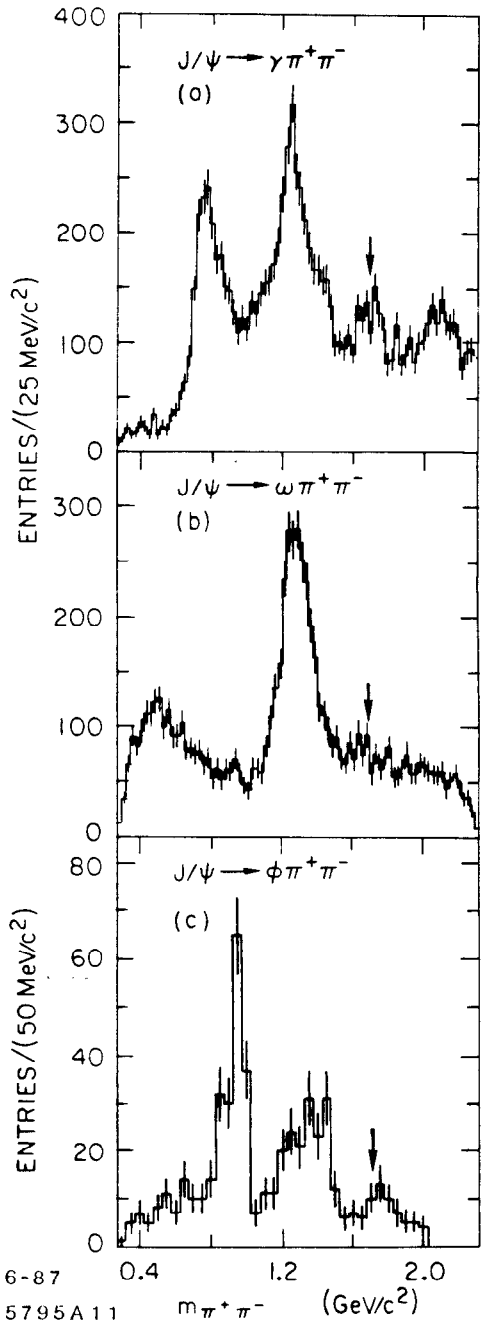

Figure 12. Mark III[2] effective mass spectra in the reactions (a) $J/\psi \rightarrow \gamma\pi^+\pi^-$, (b) $J/\psi \rightarrow \omega\pi^+\pi^-$, (c) $J/\psi \rightarrow \phi\pi^+\pi^-$.

Part b) of the figure 12 shows the $\pi\pi$ invariant mass spectrum recoiling against an ω. As expected from the quark correlations, a clear $f_2(1270)$ is observed; however, no structure is evident at the θ mass. In part c) of the figure we see a hint of a signal at the θ recoiling against the ϕ. The θ as a conventional $q\bar{q}$ meson would not be expected to be produced as the quark correlation is incorrect. Again, as in the case of the $\omega\theta$ decay of the J/ψ, DOZI processes may be contributing.

Figure 13 shows recent results of the LASS spectrometer[4] on $K^-p \to K_sK_s\Lambda$, where the invariant K_sK_s mass distribution is plotted, superimposed on the same final state produced in radiative J/ψ decays. The relative normalization is arbitrary, and has value 0.127× (LASS data) = Mark III data. The spectra match notably including the region of the $f_2'(1525)$, except in the region of the θ. A strong signal appears in the Mark III data, and none is seen in the LASS spectrum. Again this is evidence that the θ is not a convensional $q\bar{q}$ meson.

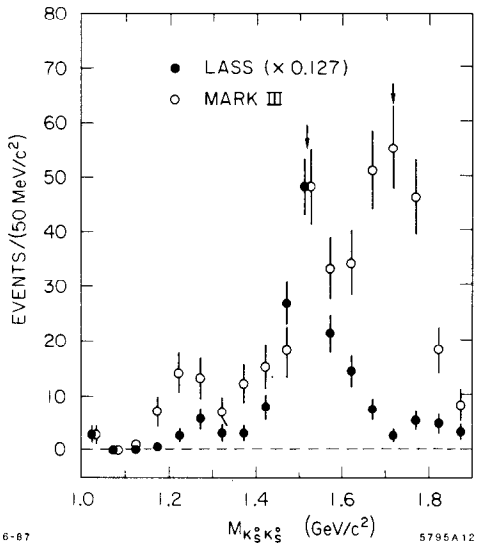

Figure 13. K_sK_s mass distributions from (open circles) Mark III uncorrected $J/\psi \to \gamma K_sK_s$ data and (solid circles) LASS acceptance corrected $K^-p \to K_sK_s\Lambda$ data. The LASS data have been multiplied by 0.127 to match the Mark III data in the 1525 MeV/c^2 bin. LASS used a 11 GeV/c K^- beam, and for this plot required $|t'| < 2$ (GeV/c)^2, where $t' = t - t_{\min}$.

We conclude the discussion on the θ with a firm impression that this meson is not a conventional $q\bar{q}$ meson, and is an excellent candidate for a 2^{++} gluonium state. Thus, over the last few years a seemingly hopelessly complicated situation has been largely redressed by the detailed work of a number of experiments. Consequently, the existence of two gluonium states, the ι and the θ, have probably been established (I dared not say this 4 or 5 years ago[19]), though there are a number of important details yet to come before most physicists are completely convinced.

3. The Question of the $\xi(2200)$

The Mark III announced the discovery of this narrow state about 4 years ago[20]. Though information about the ξ was reproduced and expanded[21] as the Mark III accumulated more J/ψ statistics over the following two years, confirmation from other experiments has been slow in coming. In particular, the DM2 experiment did not see the state, and quoted limits in contradiction to the Mark III results[22]. In the last year or so new actors have appeared, the LASS and GAMS experiments, with results confirming the Mark III results.

Figure 14 shows recent Mark III results on the $\xi(2200)$ obtained from their full data sample of 5.8 million J/ψ decays. Part a) of the figure shows the signal in radiative decays of the J/ψ to K^+K^-, part b) shows the signal in K_sK_s. A maximum likelihood fit of a Breit-Wigner line shape in the 1900–2600 MeV/c^2 mass region (see figure inserts) yields,

$$M_\xi = 2230 \pm 6 \pm 14 \text{ MeV/c}^2, \quad \Gamma_\xi = 26^{+20}_{-16} \pm 10 \text{ MeV/c}^2, \tag{19}$$

for the charged mode, and,

$$M_\xi = 2232 \pm 7 \pm 7 \text{ MeV/c}^2, \quad \Gamma_\xi = 18^{+23}_{-15} \pm 10 \text{ MeV/c}^2, \tag{20}$$

for the neutral mode. The measured branching ratios of the two modes are,

$$B(J/\psi \to \gamma\xi) \bullet B(\xi \to K^+K^-) = (4.2^{+1.7}_{-1.4} \times 10^{-5}), \tag{21}$$

and,

$$B(J/\psi \to \gamma\xi) \bullet B(\xi \to K_sK_s) = (3.1^{+1.6}_{-1.3} \times 10^{-5}). \tag{22}$$

The ratio of the branching ratios is consistent the ξ being an isoscalar.

The Mark III has made a preliminary spin-parity analysis to determine the J^P of the ξ. The relatively clean K_sK_s final state was used for this analysis using a maximum likelihood technique employed earlier[23] to obtain the J^P of the $f_2'(1525)$ and the $\theta(1720)[f_2(1720)]$. Figure 15 shows the $\cos\theta_K$ distributions for the various states (for comparison), where θ_K is the polar angle of a K_s with respect to the photon direction in the K_sK_s CM frame. The $\cos\theta_K$ distribution for the ξ is shown in part c) of the figure. The analysis rules out spin 0; the minimum spin is 2 with spin 4 also possible. Note that the K_sK_s system can only have even spin, positive parity.

Figure 16 shows results from the LASS experiment[4] Part a) of the figure shows an overlay of the Mark III and LASS $K^-p \to K_sK_s\Lambda$ data for the K_sK_s effective mass. The LASS data is arbitrarily re-normalized by 0.44. The two overlaid spectra agree well with quite similar looking

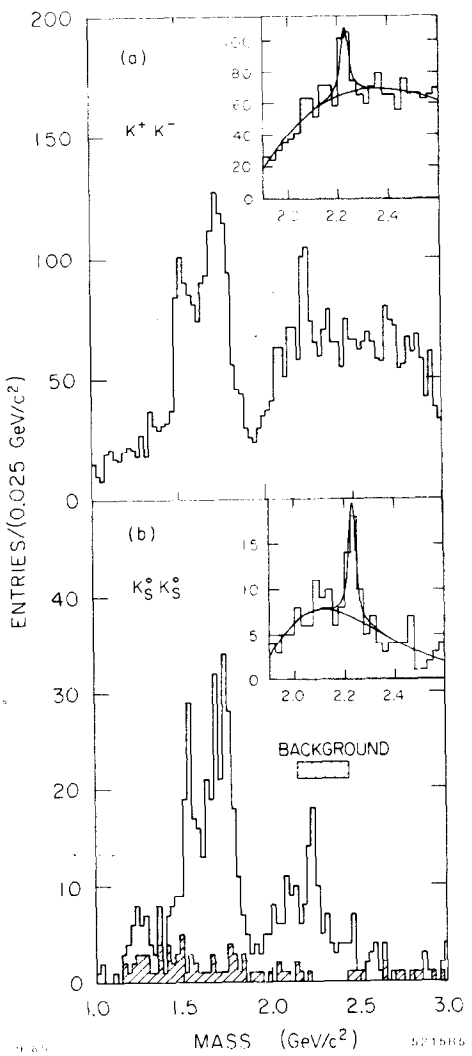

Figure 14. Mark III invariant mass distributions: Part a), K^+K^- effective mass spectrum in the radiative decay $J/\psi \to \gamma K^+K^-$; part b), K_sK_s effective mass spectrum from the decay $J/\psi \to \gamma K_sK_s$.

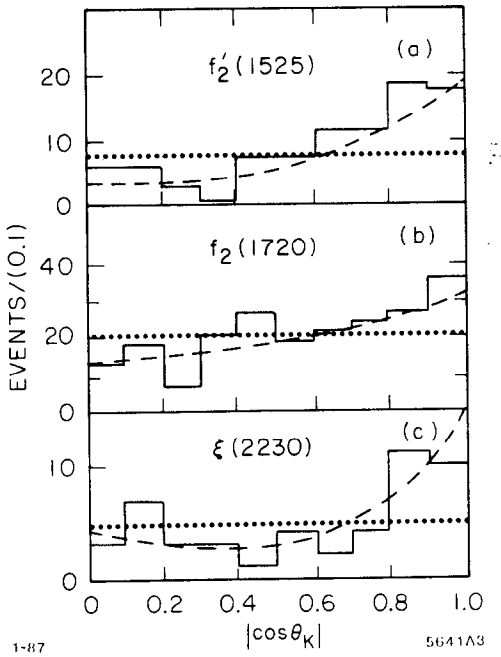

Figure 15. Mark III $\cos\theta_K$ distributions for the events in the region: a) 1420–1550 MeV/c^2, (b) 1620–1820 MeV/c^2, and (c) 2180–2280 MeV/c^2. The histograms are the data; the dotted lines are the Monte Carlo predictions for the spin 0 and the dashed lines for the spin 2 hypotheses.

structures at 2200 MeV/c^2. Results from the LASS "moment" analysis are shown in part b) of the figure. The K_sK_s invariant mass spectrum is shown for events with $\cos\theta_{GJ} > 0.85$, where θ_{GJ} is the t-channel decay angle of the K_s in the K_sK_s CM frame (see reference 4 for details). The insets in the figure show the $L = 2$ and $L = 4$, $M = 0$ moments in the 2200 MeV/c^2 mass region. Structure is seen in both moments at 2200 MeV/c^2, while moments with $L > 4$ are consistent with 0. This implies $J \geq 2$ for the ξ (again, see reference 4 for details).

The GAMS experiment[24] also reports a state at the ξ mass, seen in

$$\pi^- p \to \eta'(2\gamma)\eta(2\gamma)n. \tag{23}$$

Figure 17a),b) show the $\eta'\eta$ invariant mass obtained at two incident π^- momenta, 38 and 100 MeV/c. Structure is seen in both plots around 2200 MeV/c^2. A fit yields, $M = 2200 \pm 10$ MeV/c^2. The decay to $\eta'\eta$ implies $I^G = 0^+$. The experimenters report the observation of a "very isotropic angular distribution" which implies $J \geq 2$.

In conclusion, the two confirming experiments and the Mark III results paint a rather consistent picture of the nature of the $\xi(2200)$. The state appears to be a normal hadron with $J^P = 2^+$ or 4^+ and $I^G = 0^+$. It is narrow, though this might be explained by its spin if $J = 4$.[25] For completeness, figure 18 shows the DM2 limits[22] vs the width of the ξ. Only for $\Gamma_\xi \geq 50$ MeV/c^2 or so are the two experiments consistent.

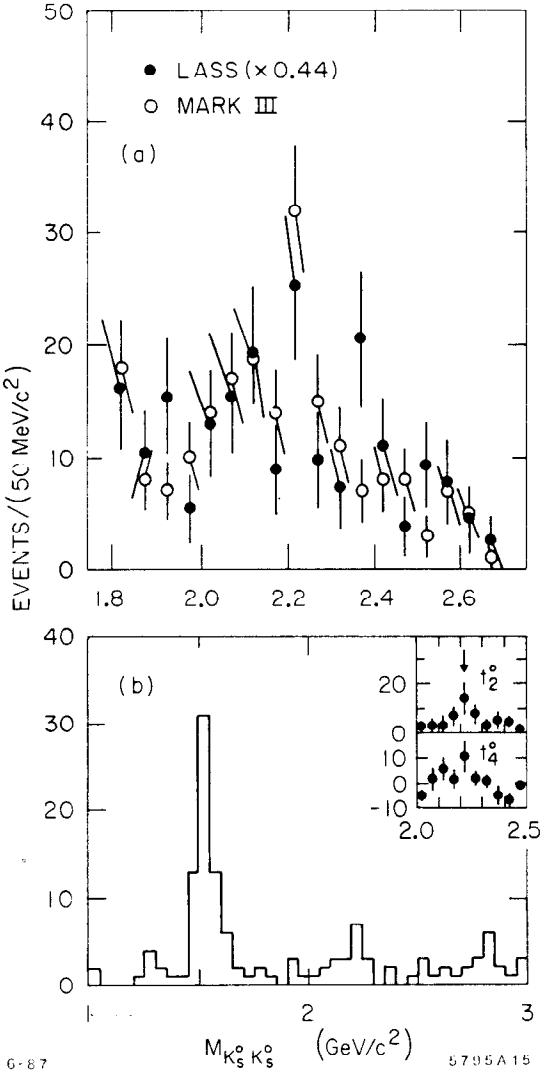

Figure 16. The LASS acceptance corrected K_sK_s invariant mass distribution: Part a), compared with the same final state produced in radiative J/ψ decay as seen by the Mark III. The solid circles are the LASS data multiplied by a factor of 0.44, the open circles are the Mark III data; part b),for events with $\cos\theta_{GJ} > 0.85$. Insets are the $L = 2$, and $L = 4$, $M = 0$ moments in the 2.2 GeV/c^2 region. Moments with $L > 4$ are consistent with 0.

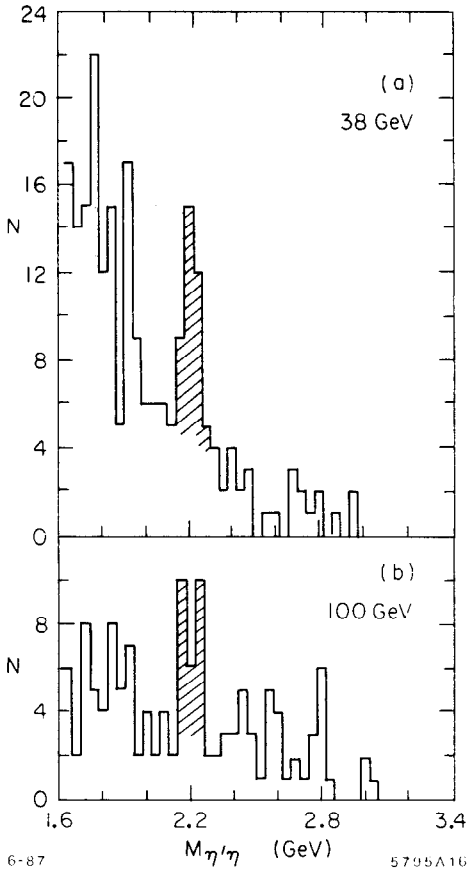

Figure 17. GAMS[27] invariant mass distribution for the final state $\eta\eta'$ from $\pi^- p \to \eta\eta' n$: (a) 38 GeV/c $\pi^- p$ data; (b) 100 GeV/c $\pi^- p$ data.

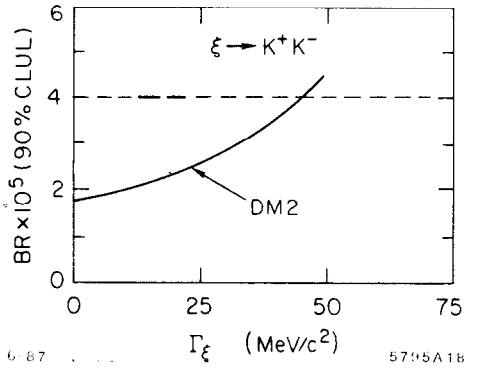

Figure 18. Upper limits from the DM2 collaboration[25] for $J/\psi \to \gamma\xi(K^+K^-)$ as a function of the width of the ξ. The dotted line is the measured value for this branching ratio from the Mark III. Only for $\Gamma_\xi \gtrsim 50$ MeV/c^2 are the two experiments consistent.

4. The Search for Radiative Decays From the Υ

The Υ, being a massive and very narrow state, may be a source of new physics. Given past experience with the J/ψ, the radiative decays of the Υ have been perceived as being particularly sensitive to new physics. Many model calculations point to the radiative decays as

a source of novel particle production, including light Higgs production[26], axion production[27], and the production of various super symmetric particles[28]. In addition, the observation of gluonium via radiative decay from the Υ was initially thought the most productive way to observe these states[29]. It is thus somewhat disheartening that after almost a decade of study not one exclusive hadronic or radiative decay mode has been observed; only limits now exist. There is clearly much to learn from Υ radiative decay, but we now know that at least an order of magnitude in experimental sensitivity, over what is presently available, is needed before the physics of these decays can be harvested.

4.1 THE SEARCH FOR $\Upsilon \to \gamma\eta$

I view this decay as the "touch stone" of the hadronic radiative decays. In some ways it is the easiest to observe, and its branching ratio should set the scale for most of the radiative decays to hadrons. This has been the case at the J/ψ. The crystal ball collaboration at DORIS II has recent results on the search for (and perhaps the first observation of ?) this decay. The analysis is based on 46 pb^{-1} of data collected on the $\Upsilon(1S)$ resonance, corresponding to about 0.5 million produced Υ mesons. Two different techniques were used for the search. One used the $3\pi^0$ decay[30], the other the 2γ decay. I will give results from both searches (and one for the $\gamma\eta'$ as well[30]), but describe only the $\eta \to 2\gamma$ in detail. These results are all preliminary.

Figure 19 schematically illustrates the appearance of the decay,

$$\begin{array}{l} \Upsilon \to \gamma + \eta \\ \qquad\quad \big\lfloor\!\!\to \gamma\gamma \end{array} \tag{24}$$

in the crystal ball detector. Typically, the pattern of energy deposition of the prompt γ produces a rounded energy cluster while that from the $2\gamma s$ (from the η decay) is oblong and somewhat irregular. These differences are subtle due to the large boost of the η, but they can be detected using specialized pattern recognition software. The CB pattern recognition routine calculates a log likelihood difference (LLD) for the 1 and 2γ hypotheses for each energy cluster; small values of the LLD imply a single γ, large positive values of the LLD imply $2\gamma s$ in the cluster. In addition, an energy cluster "mass," $M_{\gamma\gamma}$ is calculated for each cluster. Monte Carlo studies indicate that this technique has a high efficiency for detecting ηs in the $\gamma\eta(2\gamma)$ final state, and strongly suppresses the QED backgrounds, primarily $e^+e^- \to 3\gamma$.

The cuts are very simple in this analysis:

- Select 2 neutral energy clusters each with $|\cos\theta_z| < 0.75$ (well in the tracking chamber acceptance of the detector), and each having an energy consistent with E_{beam}. (θ_z is the angle to the e^+ beam.)

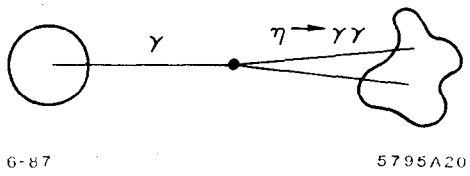

Figure 19. Representation of the energy cluster shape characteristics in the crystal ball detector for the decay $\Upsilon \rightarrow \gamma\eta(2\gamma)$.

- Evaluate each cluster using the pattern recognition software described above and cut events with LLD(1) (particle 1), and LLD(2) (particle 2), both less than 4. This leaves events with 1 cluster having LLD $< 4(\gamma$ candidate), and 1 cluster having LLD $> 4(\eta$ candidate).

Figure 20 a) shows the Monte Carlo for QED (3γ), part b) the Monte Carlo for the $\gamma\eta(2\gamma)$ final state, part c) the data, after all cuts except the LLD cuts. The LLD cuts are indicated in the figure. As can be seen in the figures, these cuts remove most of the QED background, and leave a high efficiency for the $\gamma\eta$ final state. For the η candidate (LLD$>$ 4) , figure 21 shows E_γ vs $M_{\gamma\gamma}$ for, QED Monte Carlo (a), $\gamma\eta$ Monte Carlo (b), and data (c). The plots of figure 21 have two entries per event.

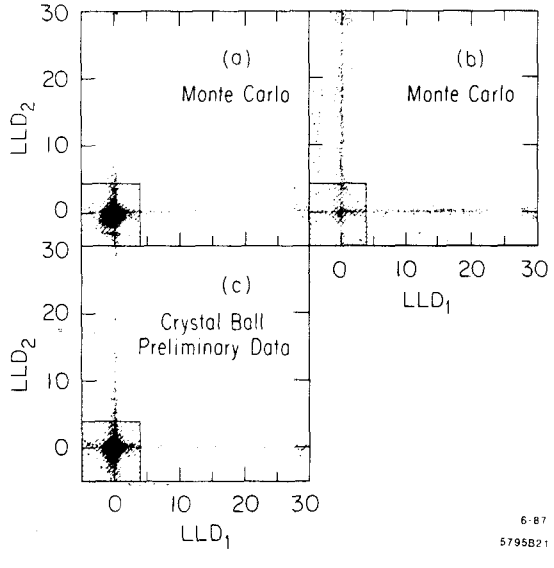

Figure 20. Log likelihood difference (LLD) for energy cluster 1 (LLD1) vs energy cluster 2 (LLD2) for the decay $\Upsilon \rightarrow 3\gamma$. Part a) is Monte Carlo for QED 3γ, part b) is Monte Carlo for $\gamma\eta(2\gamma)$, part c) is crystal ball preliminary data.

- In order to further suppress QED background, an additional cut is made shown by the solid line in figure 21c (points to the left of the dashed line are also cut as there are two entries per event).

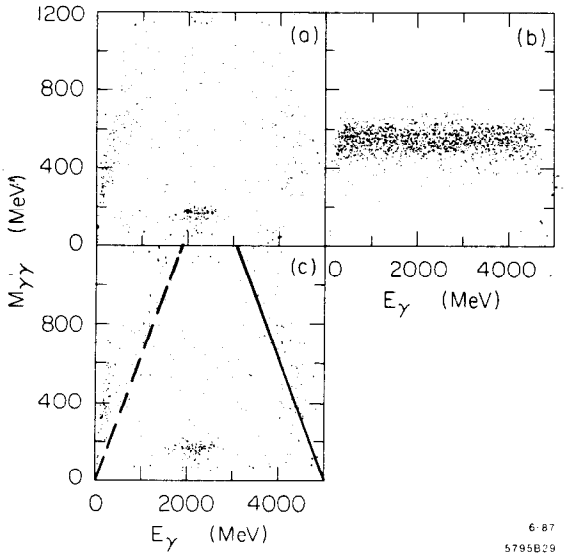

Figure 21. $M_{\gamma\gamma}$ vs E_γ for the decay $\Upsilon \rightarrow 3\gamma$ after all but the final cut. Part a) is Monte Carlo for QED 3γ, part b) is Monte Carlo for $\gamma\eta(2\gamma)$, part c) is crystal ball preliminary data. The lines on part c) represent the final cut. All data to the upper right of the solid line and upper left of the dashed line are cut. Note that part c) has two entries per event, and thus the dashed line is a reflection of the solid line.

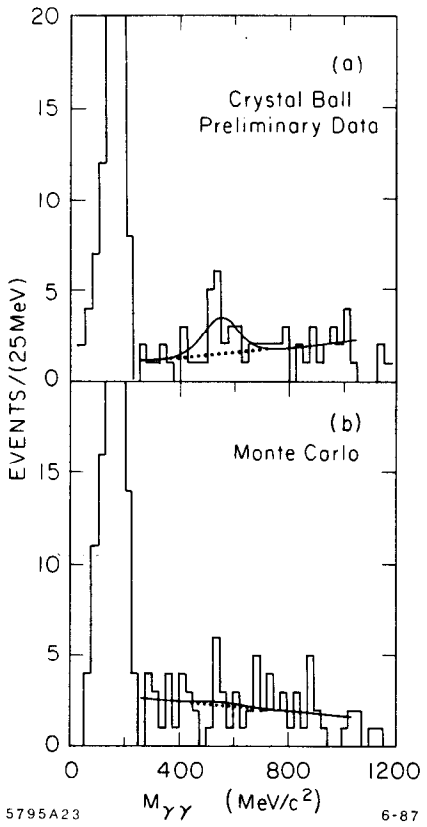

Figure 22. Preliminary Crystal Ball results for the process $\Upsilon \rightarrow 3\gamma$ after all cuts and projected to the $M_{\gamma\gamma}$ axis. Part a) is data, part b) is Monte Carlo.

The resulting events after all cuts are projected in $M_{\gamma\gamma}$ in figure 22. Part a) of this figure

shows the data, part b) QED Monte Carlo. The data shows a bump at the η mass, and a fit using the detector resolution yields, 12.4 ± 5.7 events at $M_{\gamma\gamma} = (548 \pm 28)$ MeV/c^2.

As the significance of the bump is only 2.3σ, the Crystal Ball Collaboration prefers to present the result as an upper limit (though it is tempting to call the bump a signal),

$$B(\Upsilon \to \gamma\eta) < 3.9 \times 10^{-4} (90\% \text{ C.L.}). \tag{25}$$

The crystal ball collaboration also has results from the $3\pi^0$ decay of the η which yields,

$$B(\Upsilon \to \gamma\eta) < 3.5 \times 10^{-4} (90\% \text{ C.L.}). \tag{26}$$

Figure 23 shows published results from the CLEO collaboration[31] on radiative decays to $\pi^+\pi^-, K^+K^-$, and $p\bar{p}$ final state as a function of the hadronic invariant mass. Crystal ball and CLEO results (the only available at this time) are summarized along with some theoretical comparisons in table 3 below.

Table 3.

	$\times 10^5$ $\Upsilon \to \gamma + \eta$	$\times 10^5$ $\Upsilon \to \gamma + \eta'$	$\times 10^5$ $\Upsilon \to \gamma + f_2(1270)$
Crystal Ball	$< 35(90\% \; C.L.)$	$< 130(90\% \; C.L.)$	$< 81(90\% \; C.L.)$
CLEO[31]			$< 4.8(90\% \; C.L.)$
"Theory," Section 2.	14	42	11
Dishpande, Elam[32]	15	100	—
Intemann[33]	0.06	0.25	—
Korner et al.[34]	3.4	16	14
Tye[35]	2.2	11	4
	$\psi \to \gamma + \eta$	$\psi \to \gamma + \eta'$	$\psi \to \gamma + f_2(1270)$
PPDB[36]	86 ± 8	420 ± 50	160 ± 20

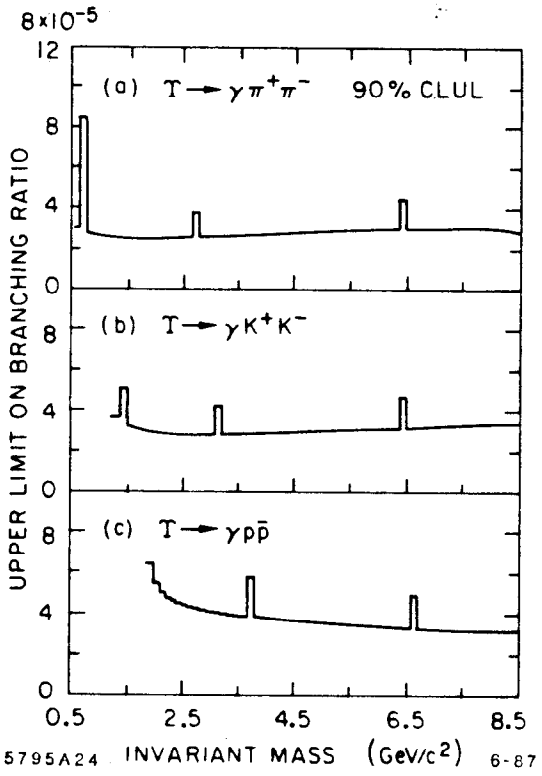

Figure 23. Results from CLEO[34] for 90% -confidence-level upper limits on branching fractions as functions of the invariant mass of the two hadrons for (a) $\Upsilon \to \gamma\pi^+\pi^-$,(b) $\Upsilon \to \gamma K^+K^-$, and (c) $\Upsilon \to \gamma p\bar{p}$, These limits assume a particle width of less than 100 MeV/c^2.

4.2 THE SEARCH FOR THE $^1S_{0_b}$ STATES

Figure 24 a), b) show crystal ball collaboration results[37] for th inclusive photon spectra from about 300k $\Upsilon(1S)$ and 193k $\Upsilon(2S)$ hadronic decays. Parts c) – e) of the figure show the limits obtained from these spectra, and limits from the CUSB collaboration[38] for radiative decay to the η_b and η_b'. The crystal ball results are preliminary. Also shown in parts c) – e) of the figure are the measured values of the corresponding transitions at the J/ψ, which have all been measured by the crystal ball[36]. The expectation of the theory appears as the solid line at the bottom of parts c) and e) of the figure (the theory for $\Upsilon(2S) \to \gamma\eta_b$, is less reliable). For example,

$$B(\Upsilon(1S) \to \gamma\eta_b) \simeq 0.1\% \times (E_\gamma/100\ \text{MeV})^3. \tag{27}$$

The experiments are not yet close to the theoretical predictions for the expected masses of the $^1S_{0_b}$ states. About a factor of 10 is needed in sensitivity.

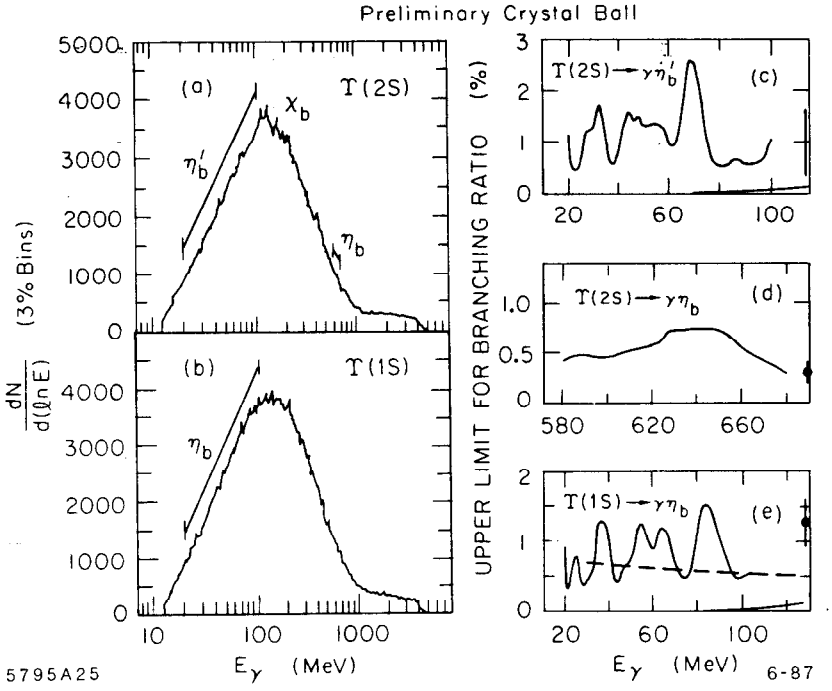

Figure 24. Preliminary results from the crystal ball. a) the inclusive photon spectrum from the $\Upsilon(2S)$, b) the inclusive photon spectrum from the $\Upsilon(1S)$, c) – e) 90% -confidence-level upper limits from radiative decay of the $\Upsilon(1S)$ and $\Upsilon(2S)$ into η_b and η_b' as indicated in each figure vs the energy of the inclusive photon. The data point on the right of each sub-figure is the crystal ball measurement of the process at the J/ψ.

4.3 The Search for the Higgs.

For low enough mass, the standard Higgs boson was predicted to have a radiative branching ratio of about 10^{-4} from the $\Upsilon(1S)$. More recent predictions, including higher order QCD effects, have dropped the theoretical values by about a factor of 2[39]. As very few experimental limits exist on standard Higgs production, much effort from the crystal ball[40] and CUSB[41] collaborations has gone into setting experimental limits in $\Upsilon(1S)$ radiative decay to a Higgs. Figure 25 shows the results of these searches. The experimental limits are the upper solid lines, the theories the lines below. For the most recent theory, the bottom line in the figures, more than a factor of 10 in sensitivity is needed by the experiments to exclude the standard Higgs over most of the available mass range. For a very light Higgs, about 3 GeV/c^2 and below, perhaps a factor of 4 in sensitivity will suffice. The CUSB collaboration, with a new BGO detector, hopes to continue the search to the requisite level of sensitivity to exclude a standard Higgs over most of the mass range allowed via $\Upsilon(3S)$ radiative decay[42]. They expect sufficient data by the end of the decade.

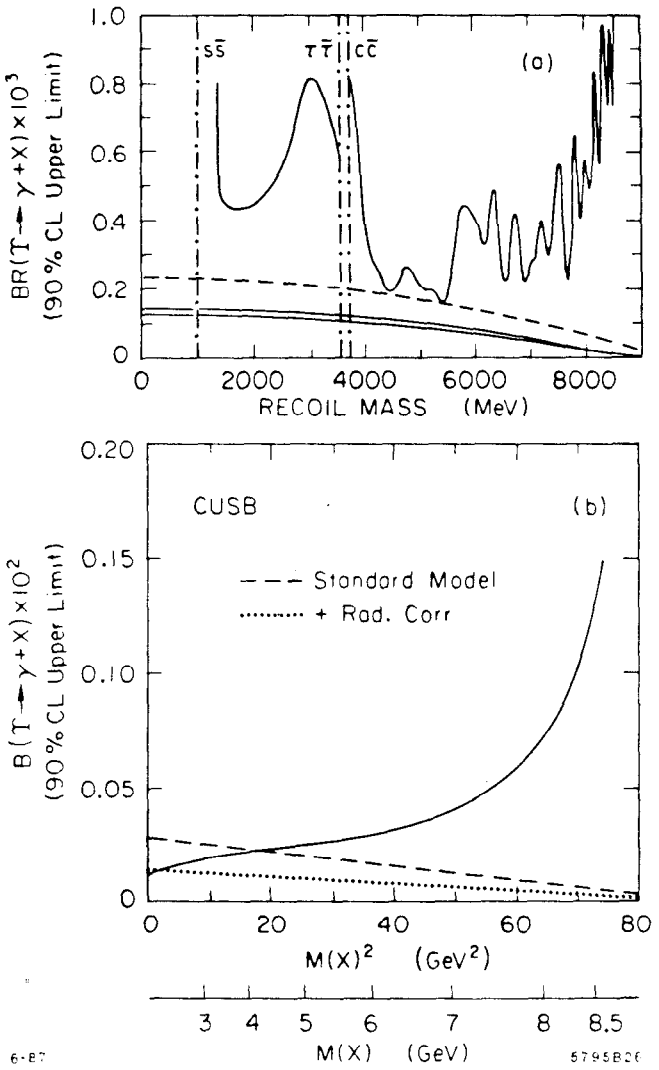

Figure 25. Limits on $\Upsilon(1S) \rightarrow \gamma X$ compared to standard model calculations for $\Upsilon \rightarrow \gamma$ Higgs. a) preliminary results from the crystal ball. The vertical dashed-dot lines show the kinematic thresholds for the relevant fermions. The horizontal dashed line corresponds to the lowest order calculation for the Wilczek mechanism. The two solid lines (roughly horizontal) indicate the range of the theoretical estimate of the first order QCD radiative corrections to the Wilczek calculation. b) similar published results from the CUSB experiment. The top solid is a smoothed experimental limit, the bottom two lines are theory as indicated in the figure.

As mentioned above, $\Upsilon(nS), n = 1 - 3$, radiative decays are considered fertile ground for exotic particle searches due to the large masses and narrow widths of these states, Examples of such searches are shown in figures 26 and 27. Figure 26 shows preliminary results from the crystal ball collaboration on the decay,

$$\Upsilon(2S) \rightarrow \pi^0\pi^0\Upsilon(1S) \qquad \hookrightarrow \gamma + \text{Unseen}, \tag{28}$$

where Unseen is a long lived, noninteracting particle. Part a) of figure 26 shows the counts/10 MeV vs E_γ remaining after all cuts in the crystal ball analysis. Part b) of the figure shows the resulting 90% C.L. branching ratio for the radiative decay of the Υ to a noninteracting particle. Part c) of the figure shows the dependence of the branching ratio limit on the lifetime of the particle (vs the unseen particle mass) assuming the unseen particle decays into some particles that interact. This analysis is continuing and will include a search for unseen particles from direct decays of the $\Upsilon(1S)$ as well as a search for radiative decays containing a γ and multiple unseen particles.

Figure 27 shows results from the CUSB collaboration[43] searching for,

$$\Upsilon(1S) \rightarrow \gamma + (\tilde{g}\tilde{g}), \tag{29}$$

where the two gluinos are in a bound state, gluinium[43]. Figure 27 a) shows the results of two theoretical calculations[44,45] of the radiative branching ratio to gluinium states vs half the mass of the bound state (taken as the gluino mass). The experimental upper limit from CUSB is also shown in the figure. No indication for gluinium states are seen resulting in a model dependent limit on the gluino mass. An important virtue of this gluino mass limit is its non-dependence on the squark mass as shown in figure 27 b), where the CUSB limit is compared to gluino mass limits from other experiments.

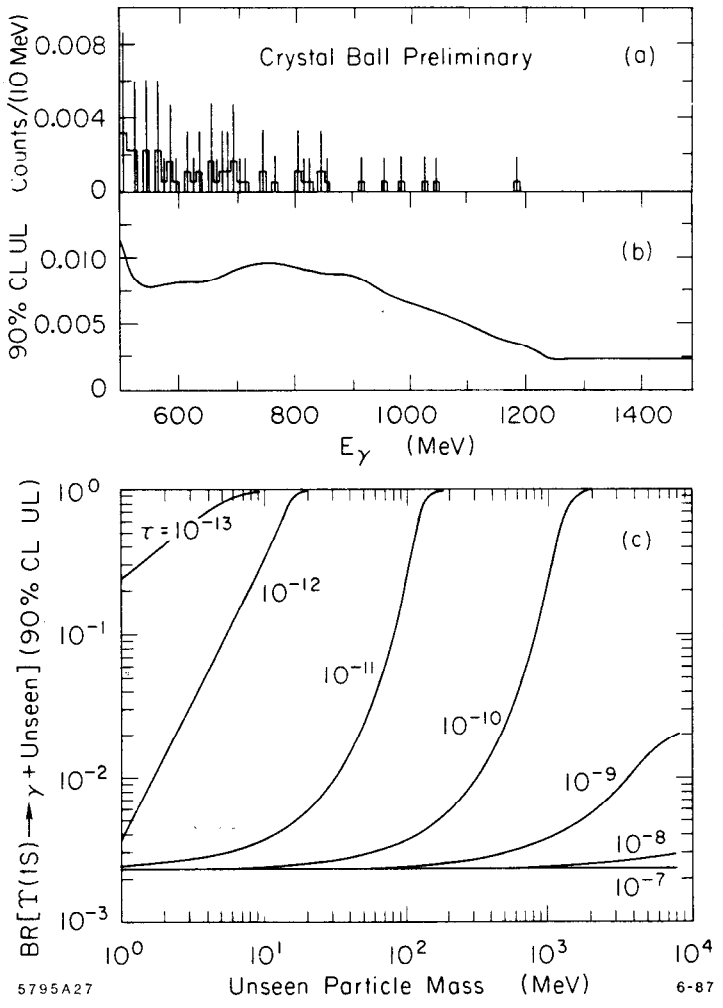

Figure 26. Preliminary results from the crystal ball for $\Upsilon(2S) \rightarrow \pi\pi\Upsilon(1S)$, $\Upsilon(1S) \rightarrow \gamma$ Unseen. a) the corrected photon spectrum. b) the 90% -confidence-level upper limits derived from the spectrum in a) assuming a long lived non-interacting particle. c) the limits as a function of the lifetime (τ) of the unseen particle assuming that some of its decay products interact.

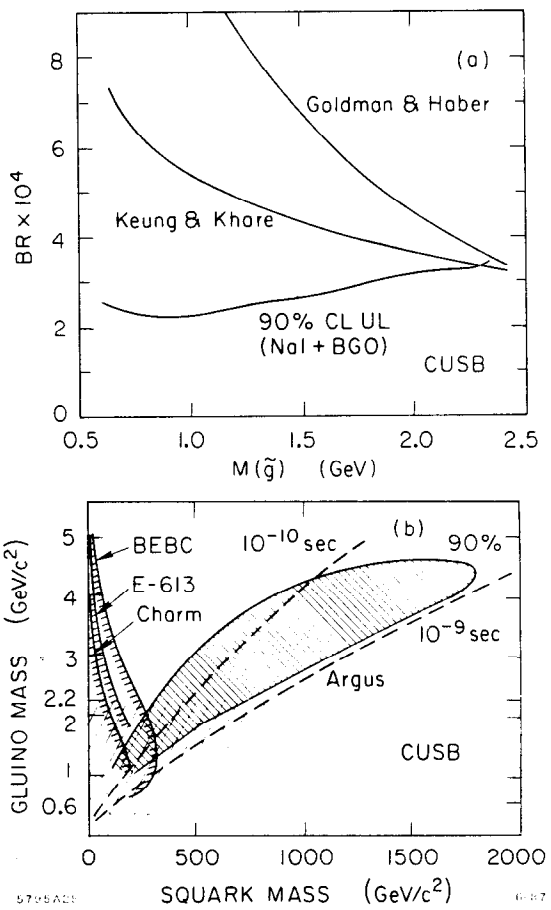

Figure 27. a) CUSB 90% -confidence-level upper limits (bottom curve) compared to two theoretical models for $\Upsilon \rightarrow \gamma$ gluinium. The abscissa is taken as half the gluinium mass. This limit results in a model dependent gluino mass limit. b) CUSB gluino mass region excluded together with beam dump and ARGUS results.

5. Future Perspectives

Though much has been accomplished on the untangling of the gluoinium spectroscopy, much is left to be done. It is clear by this time that the J/ψ, and perhaps the ψ' present powerful tools to analyze and extract the complex $q\bar{q}$, gg (and $gq\bar{q}$) spectroscopes of the low mass hadronic states. In order to continue the progress of the last 5 years, new facilities, both machines and detectors are needed. The Beijing machine holds promise in this respect; however, the complexity and difficulty of the problems demand confirmation of results from more than one experiment and preferably from different laboratories.

As the progress has been promising in the case of the J/ψ system over the past years, it has been somewhat disappointing in the Υ system over a similar time frame. The match of detectors and machines has not been as powerful a tool. In the case of Υ physics (and B meson physics), the systematic study of these states has barely begun. Remember, not one exclusive hadronic decay of the Υ is presently known. The study of gluonium spectroscopy at the Υ is still to be started. The searches for exotics, especially the Higgs, need an order of magnitude in sensitivity to reach the level of standard model theoretical predictions. What is required here is a B factory capable of producing 10–20 Million $\Upsilon(1S), \Upsilon(2S), \Upsilon(3S)$ events as well as 10–20 Million B meson decays in a reasonable time. Such a machine would not only greatly improve our knowledge of Υ decays, it could also be used for important tests of the standard model in other areas such as B meson mixing, and perhaps a measurement of CP violation in the B meson system. If attained, the latter goal alone would justify building such a B Factory.

ACKNOWLEDGEMENTS

I would like to thank members of the crystal ball collaboration, particularly, Susan Cooper, Kay Königsmann, and Steve Lowe for their input while I was preparing this talk. Usha Mallik of the Mark III collaboration and Blair Radcliff of the LASS collaboration were unusually helpful and patient in explaining the intricacies of the results from their respective collaborations. Finally, I would like to thank the organizers of this stimulating conference, Giorgio Bellettini and Mario Greco, for an excellent setting as well as interesting and timely content.

REFERENCES

[1.] C. Baflin et al. (R704), Phys. Lett. **171B**, 135 (1986).

[2.] U. Malik, SLAC-PUB-4238 (1987).

[3.] a) H. Aihara, et al., Phys. Rev. Lett. **57**, 51 (1986);
b) H. Aihara, et al., Phys. Rev. Lett. **57**, 2500 (1986).

[4.] D. Aston, et. al., SLAC-PUB-4202, (1987).

[5.] H. Albrecht et al. (ARGUS Collab.), Contributed paper to the 23rd International Confernce on HEP, 1986, Berkeley; T. Bowcock et al., Phys. Rev. Lett. **56**, 2676 (1986); G. Margeras et al., Phys. Rev. Lett. **56**, 2672 (1986).

[6.] C. Edwards et al., Phys. Rev. Lett. **48**, 903 (1982).

[7.] S. Brodsky et al., Phys. Lett. **73B**, 203 (1978).

[8.] A. Ore and J. L. Powell, Phys. Rev. **75**, 1696 (1949).

[9.] G. S. Abrams et al., Phys. Rev. Lett. **44**, 114 (1980) and Phys. Rev D **23**, 43 (1981).

[10.] R. D. Schambergr et al., Phys. Lett. **138B**, 225 (1984).

[11.] S. E. Csorna et al., Phys. Rev. Lett. **56**, 1222 (1986).

[12.] E. D. Bloom and F. J. Gilman, Phys. Rev. D **4**, 2901 (1971).

[13.] A. Billoire, R. Lacaze, A. Morel and H. Navelet, Phys. Lett. **80B**, 381 (1979); J.G. Körner, J.H. Kühn, M. Krammer and H. Schneider, Nucl. Phys. **B229**, 115 (1983).

[14.] P. Baillon et al., Nuovo Cimento **50A**, 393 (1967); S. U. Chung et al. Phys. Rev. Lett. **55**, 770 (1985); A. Ando et al., KEK Report No. 86–8, 1986 (to be published); D. F. Reeves et al., Phys. Rev. D **34**, 1960 (1986)

[15.] M. Chanowitz, Phys. Rev. Lett. **187B**, 409 (1987).

[16.] J. J. Becker et al., SLAC-PUB-4149, to appear in Phys. Rev. Lett. (1987).

[17.] M. Stanton et al., Phys. Rev. Lett. **42**, 346 (1979); A. Ando et al., Phys. Rev. Lett. **57**, 1296 (1986).

[18.] F. M. Renard, Nuovo Cimento **80A**, 1 (1984). Also see reference 14 contained in reference 3b.

[19.] E. D. Bloom, 21st Int. Conference on High Energy Physics, Paris, France, July 26–31, 1982, J. Phys. **C3**, Suppl. 12, 407 (1982).

[20.] K. Einsweiler, Proceedings of the International Europhysics Conference on High Energy Physics, Brighton, (1983); W. Toki, Proceedngs of the 11th SLAC Summer Institute on Particle Physics, July (1983); D. Hitlin, Proceedings of the International Symposium on Lepton and Photon Interactions, Cornell, (1983).

[21.] R. M. Baltrusaitis et al., Phys. Rev. Lett. **56**, 107 (1986).

[22.] J. E. Augustin et al., Orsay preprint, LAL/85–27, (1985); B. Jean-Marie (DM2 collaboration), Proceedings of the XXIII International Conference on High Energy Physics, Berkeley, California, July 16–23, 1986, Editor S. Loken, **652**, (1987).

[23.] J.J. Becker et al., SLAC-PUB-4149, to appear in Phys. Rev. Lett. (1987).

[24.] F. Binon (GAMS collaboration), Proceedings of the XXIII International Conference on High Energy Physics, Berkeley, California, July 16–23, 1986, Editor S. Loken, **700**, (1987).

[25.] S. Godfrey, R. Kokoski and N. Isgur, Phys. Lett. **141B**, 439 (1984).

[26.] F. Wilczek, Phys. Rev. Lett. **39**, 1304 (1977).

[27.] For a review of axion production in quarkonium decays see, W. Buchmüller and S. Cooper, MIT-LNS-159 (1987).

[28.] For a review of supersymmetric particle production in quarkonium decays see, J. H. Kühn, Acta Physica Polonica **B16**, 969 (1985).

[29.] K. Koller, T. Walsh, Nucl. Phys. **B140**, 449 (1978); also reference 7.

[30.] P. Schmitt (crystal ball collaboration), Universität Wurtzburg Ph.D. thesis, to be published (1987).

[31.] A. Bean et al., Phys. Rev. D **34**, 905 (1986).

[32.] N. G. Deshpande and G. Eilam, Phys. Rev. D **25**, 270 (1982).

[33.] G. W. Intemann, Phys. Rev. D **27**, 2755 (1983).

[34.] J.G. Körner, J.H. Kühn, M. Krammer and H. Schneider, Nucl. Phys. **B229**, 115 (1983).

[35.] S.H. Tye, Proc. 1982 DPF Summer Study on Elementary Particle Physics and Future Facilities, Snowmass, Colorado, Editors R. Donaldson, R. Gustafson, and F. Paige, 197 (1983).

[36.] Particle Properties Data Booklet, Phys. Lett. **170B**, (1986).

[37.] R. T. Van de Walle (crystal ball collaboration), Proceedings of th XXIII International Conference on High Energy Physics, Berkeley, California, July 16-23, 1986, Editor S. Loken, **677**, (1987).

[38.] J. Lee-Franzini, Proceedings of the Conference on Physics in Collision 5, Autun, France, July, 1985.

[39.] F. Wilczek, Phys. Rev. Lett. **39**, 1304 (1977); M. I. Vysotsky, Phys. ett. 97B, 159 (1980); J. Ellis et al., Phys. Lett. **158B**, 417 (1985).

[40.] S. T. Lowe (crystal ball collaboration), Stanford Univesity Ph. D. Thesis, SLAC Report - 307, (1986).

[41.] P. Franzini et al., contributed paper 312 to the 1985 International Symposium on Lepton and Photon Interactions at High Energy, Kyoto, Japan (1985); P. Franzini et al., submitted for publication to Phys. Rev. D. Brief reports; S. Youssef et al., Phys. Lett. **39B**, 332 (1984).

[42.] P. M. Tuts, private communication.

[43.] P. M. Tuts, Proceedings of the XXIII International Conference on High Energy Physics, Berkeley, California, July 16–23, 1986, Editor S. Loken, 609 (1987) .

[44.] T. Goldman and H. Haber, Los Alamos Preprint LA-UR-84-634 (1984).

[45.] W.-Y. Keung and A. Khare, Phys. Rev. D **29**, 2657 (1984).